Analytica Chimica Acta 850 (2014) 33–40

Contents lists available at ScienceDirect

Analytica Chimica Acta

journal homepage: www.elsevier.com/locate/aca

A label-free and high sensitive aptamer biosensor based on hyperbranched polyester microspheres for thrombin detection

Chong Sun [a,b], Qiaorong Han [a], Daoying Wang [b], Weimin Xu [b], Weijuan Wang [a], Wenbo Zhao [a,*], Min Zhou [c,**]

[a] Jiangsu Key Laboratory of Biofunctional Materials, Biomedical Functional Materials Collaborative Innovation Center, College of Chemistry and Materials Science, Nanjing Normal University, Nanjing 210023, China
[b] Institute of Agricultural Products Processing, Jiangsu Academy of Agricultural Sciences, Nanjing 210014, China
[c] Department of Vascular Surgery, the Affiliated Drum Tower Hospital of Nanjing University Medical School, Nanjing 210008, China

HIGHLIGHTS

- A label-free thrombin aptamer biosensor applied in whole blood has been developed.
- The aptamer biosensor showed a wide detection range and a low detection limit.
- The antibiofouling idea utilized for biosensor is significant for diagnostics.

GRAPHICAL ABSTRACT

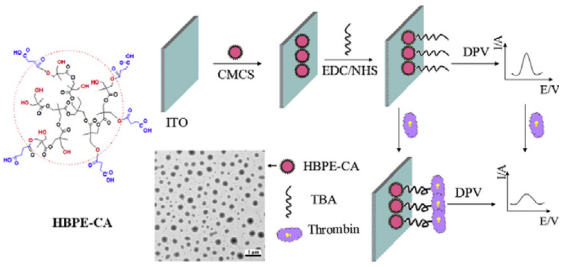

ARTICLE INFO

Article history:
Received 14 July 2013
Received in revised form 6 August 2014
Accepted 7 August 2014
Available online 11 August 2014

Keywords:
Hyperbranched polyester microspheres
Whole blood
Antibiofouling
Aptamer biosensor
Thrombin

ABSTRACT

In this paper, we have synthesized hyperbranched polyester microspheres with carboxylic acid functional groups (HBPE-CA) and developed a label-free electrochemical aptamer biosensor using thrombin-binding aptamer (TBA) as receptor for the measurement of thrombin in whole blood. The indium tin oxide (ITO) electrode surface modified with HBPE-CA microspheres was grafted with TBA, which has excellent binding affinity and selectivity for thrombin. Binding of the thrombin at the modified ITO electrode surface greatly restrained access of electrons for a redox probe of $[Fe(CN)_6]^{3-/4-}$. Moreover, the aptamer biosensor could be used for detection of thrombin in whole blood, a wide detection range (10 fM–100 nM) and a detection limit on the order of 0.90 fM were demonstrated. Control experiments were also carried out by using bull serum albumin (BSA) and lysozyme in the absence of thrombin. The good stability and repeatability of this aptamer biosensor were also proved. We expect that this demonstration will lead to the development of highly sensitive label-free sensors based on aptamer with lower cost than current technology. The integration of the technologies, which include anticoagulant, sensor and nanoscience, will bring significant input to high-performance biosensors relevant to diagnostics and therapy of interest for human health.

1. Introduction

Thrombin, a kind of serine protease, plays an essential role in some physiological and pathological processes, such as blood solidification, wound cicatrisation and inflammation [1]. The concentration of thrombin in blood varies considerably and can be virtually absent in healthy subjects. However, in the coagulation

* Corresponding author. Tel.: +86 25 85891635; fax: +86 25 83598280.
** Corresponding author.
E-mail addresses: zhaowenbo@njnu.edu.cn (W. Zhao), zhouminnju@126.com (M. Zhou).

http://dx.doi.org/10.1016/j.aca.2014.08.010
0003-2670/

process, the concentration of thrombin in blood ranges from nM to low mM levels [2,3]. Therefore, the specific recognition and quantitative detection of thrombin is extremely crucial to fundamental research as well as to clinical practice. Electrochemical [4,5] and optical techniques [6,7] were widely applied for thrombin detection. Aptamers are artificial oligonucleic acids to bind specific target molecules, which are in vitro selected by SELEX (systematic evolution of ligands by exponential enrichment) technology [8,9]. Theoretically, it is possible to obtain all kinds of aptamers to recognize virtually different target molecules with high affinity and specificity. Aptamers used for specific protein binding studies have drawn much interest recently [10–15], especially for thrombin [4,5,16,17]. However, as we know, the detection methods of thrombin concentration are mainly performed in serum which is isolated from whole blood [18,19]. When the electrode surface is contact with blood directly, the foreign materials are prone to initiate the formation of clots, as platelets and other components of the blood coagulation system are activated. At present, it is very difficult to design and prepare an electrochemical biosensor that can be used in whole blood just because the biofouling of electrode surface can be developed by platelet, fibrin and blood cell adhesion in the complex environment of whole blood media. The focus of this paper is the development and investigation of antibiofouling properties of new nanostructured architecture for electrochemical aptamer biosensors that can be applied in whole blood directly.

Hyperbranched polymers have attracted significant attention for their unique architecture and novel properties including good solubility, special viscosity behavior, and high density of their functional groups [20,21]. Owing to the multifunctionality in hyperbranched polymers, the physical properties can be adjusted to a large extent by the chemical modification of the terminal-groups [22,23]. The use of hyperbranched polymers by the chemical modification has attracted increasing attention in recent years [24–27]. At present, the original material of hyperbranched polyester (HBPE) can only be dissolved in organic solvent (e.g., dimethyl sulphoxide (DMSO), tetrahydrofuran (THF)) and not in water which is not suitable for meeting bioapplications. In this paper, we synthesized water-soluble microspheres by the chemical modification of aliphatic HBPE with carboxylic acid functional groups (HBPE-CA). The preparation and blood compatibility of the HBPE-CA microspheres were investigated. Moreover, a label-free and sensitive aptamer biosensor based on the HBPE-CA microspheres was prepared due to the coherence between blood compatibility and antifouling property which in our knowledge has never been reported. Meanwhile, the aptamer biosensor showed a wide detection range and a low detection limit. More details were presented.

2. Experiments

2.1. Materials

Thrombin-binding aptamer (TBA) was purchased from Sangon Biotechnology Co., Ltd. (China) with HPLC purification. The 5′-terminus of TBA contained 15 bases with its sequence as follows: 5′-NH_2-GGT TGG TGT GGT TGG-3′. Thrombin (human α-Thrombin), *N*-ethyl-*N*′-(3-dimethylaminopropyl) carbodiimide (EDC) and *N*-hydroxysuccinimidobiotin (NHS) were obtained from Sigma–Aldrich (USA). Carboxymethyl chitosan (CMCS), bull serum albumin (BSA) and lysozyme were purchased from Aladdin Chemistry Co., Ltd. (China). Butanedioic anhydride was purchased from Energy Chemical Co., Ltd. (China). Triethylamine, THF and crystal violet were purchased from Sinopharm Chemical reagent Co., Ltd. (China). Meanwhile, triethylamine and THF were refluxed with CaH_2 and sodium respectively, then distilled prior to use. Other reagents were used without further purification. All solutions were prepared with double-distilled water and high purity N_2 was applied for deaeration. Phosphate buffer solution (PBS) was prepared with 0.1 M NaH_2PO_4 and 0.1 M Na_2HPO_4 solutions. The ITO electrodes were purchased from Zhongjingkeyi Technology Co., Ltd. (China).

2.2. Instrumentation

Proton nuclear magnetic resonance spectroscopy (^{1}H NMR) experiment was performed on a Bruker Avance 400 spectrometers (Bruker, Germany) with D_2O as solvent at ambient temperature. The chemical shifts were referenced to tetramethylsilane (TMS) standard. The electro-spray ionization mass spectrometry (ESI-MS) was obtained from mass spectrometer (LCQ/M/Z = 150–2000, Finnigan, USA). Transmission electron microscopy (TEM) image was obtained using an interface high-resolution transmission electron microscopy (HITACHI H-7650, Japan).

2.3. Procedures

2.3.1. Synthesis of HBPE-CA microspheres

The HBPE-CA microspheres were prepared by a procedure described in the previous literatures [28]. In brief, the hyperbranched polymer HBPE (1.02 g with 0.87 mM —OH groups) was dissolved in 60 mL THF. Then 2.07 g butanedioic anhydride and 1.0 mL triethylamine were dissolved in 40 mL THF and added into the polymer solution. The reaction mixtures were stirred at room temperature for 20 h. Upon completion, white viscous products were filtrated on the bottom of the flask and the solvent was removed. After the viscous products were dissolved in ethanol and precipitated with THF for three times, the filtrate was washed by THF for several times, then the hyperbranched polyester HBPE-CA microspheres were obtained. Yield 80%.

2.3.2. Hemocompatibility evalution of HBPE-CA microspheres

The coagulation assays were performed and measured by using a Semi automated Coagulometer (RT-2204C, Rayto, USA). Expression of the fluorescently labeled platelet activation marker anti-CD62P and the platelet pan-marker anti-CD42a was detected using a BD FACSCalibur (BD Biosciences, USA). All the platelet activation experiments were done in triplicates.

2.3.3. Preparation of the HBPE-CA microspheres modified GCE

Prior to each experiment, the indium tin oxide (ITO) electrodes with dimension of 2 cm × 0.5 cm were sonicated alternately with chemical detergent solution, deionized water, acetone and ethanol, each for 10 min to get clean ITO surface. After rinsing with ethanol and drying with N_2 stream, 1/3 part of the ITO electrode was immersed in the mixture of CMCS and HBPE-CA (V/V = 1/4). The modification process of the electrode was shown as Scheme 1. CMCS was chosen as an adhesive molecule to immobilize HBPE-CA on the clear surface of the ITO electrode, and dried in the air freely. The HBPE-CA modified ITO electrode was immersed in 0.10 M PBS (pH 7.4) which contained EDC and NHS as a coupling agent for about 16 h to activate the carboxyl-terminated surface of the HBPE-CA [29], followed by rinsing with PBS and dried with N_2. Then the ITO electrode was immersed in PBS (pH 7.4) containing 1 μM TBA at 4 °C for 24 h, followed by rinsing with PBS and dried with N_2 again. Here, TBA was molecularly grafted onto the surface of modified GCE via covalent binding. After blocking the nonspecific binding sites by 1% BSA, such prepared ITO electrode was incubated with thrombin. The control experiment employed to detect thrombin in human serum was followed according to the literature [30]. First, the fluorescence spectra of crystal violet were recorded on a fluorometer (Cary Eclipse, Varian, USA) with

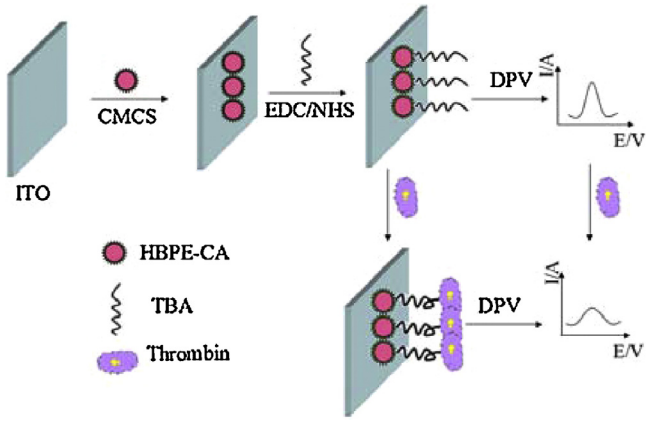

Scheme 1. The modification process of the thrombin/TBA/(HBPE-CA) modified ITO electrode.

excitation at 590 nm and an emission range from 615 to 750 nm. Then, a certain volume of 1 μM TBA was added into the 5 mM crystal violet solution. The fluorescence of this mixture was recorded after incubating for 30 min. For the study of thrombin interaction with crystal violet, the solutions of thrombin in the range of 0.001–0.1 μM were added into the above mixture for fluorescence detection.

2.3.4. Characterization of TBA/(HBPE-CA) hybrids

The existence of HBPE-CA microspheres and TBA/(HBPE-CA) was detected by an UV–vis spectrophotometer (Cary 50 Conc, Australia). Circular dichroic (CD) spectra of DNA oligonucleotides were measured for 1 μM TBA concentration using an Applied Photophysics Chriascan circular dichroism spectrometer at room temperature. CD spectra were recorded using a quartz cell of a 1 cm optical path length and an instrument scanning speed of 50 nm min^{-1} at room temperature. CD spectra were obtained by taking the average of three scans made from 200 to 320 nm. All DNA samples at a final concentration of 1 μM were dissolved in 0.10 M PBS (pH 7.4).

TBA and TBA/(HBPE-CA) hybrids samples were prepared by premixing 6 × orange DNA loading dye to a concentration of about 125 μM. After the 16 cm × 16 cm × 0.1 cm gel (20%, the mono:bis ratio was 29:1) was formed, 10.0 μL of the samples were added to each lane. Electrophoresis was carried out with a constant volt of 100 V for 12 h under 1 × TBE buffer, stained by SYBR Green I for 30 min, and then the gel image was captured.

2.3.5. Electrochemical measurements

A normal three-electrode configuration consisting of a modified ITO working electrode, a saturated calomel electrode (SCE) reference electrode and a platinum wire auxiliary electrode was used. Cyclic voltammetry (CV) was performed on a CHI 760D electrochemical analyzer (Shanghai Chenhua, China) in 0.10 M PBS (pH 7.4) containing 10 mM $K_3Fe(CN)_6/K_4Fe(CN)_6$ and 0.1 M KCl by scanning the potential between −0.4 and 1.0 V. The parameters applied in differential pulse voltammetry (DPV) were as follows: pulse amplitude of 50 mV, pulse width of 50 ms and voltage range from −0.12 to 0.55 V. The electrochemical impedance spectroscopy (EIS) tests were carried out in the frequency range of 0.1 Hz–10 kHz with 5 mV AC amplitude. The data points were taken after 2 s quiet time (12 data points per frequency decade). All measurements were carried out at room temperature. To examine regeneration of the aptamer biosensor, the aptamer electrode was rinsed with 7 M urea solution and 25 mM Tris–HCl buffer solution two times to break the interactions between TBA and thrombin. The beacon aptamer was subsequently heated to 90 °C for 1 min, and allowed to cool in ice for 10 min, respectively. After the cooling step, the beacon aptamer was incubated with thrombin solution again, and subsequently washed. Using DPV, the signal change was observed before and after target binding. The measurements were repeated four times.

Scanning electron microscopy (SEM) was used to characterize the stepwise fabrication process of the aptamer biosensor. The SEM micrographs were collected under high vacuum with an accelerating voltage of 20 kV using a JEOL JSM-6300 scanning electron microscope. All substrates were treated by the same modification process at the ITO surface and were fixed on the disks. The disks were rinsed, air-dried, coated with gold, and then the surface was investigated by SEM.

3. Results and discussion

3.1. Characterization of the HBPE-CA microspheres

Hyperbranched polymers composed of densely branched structures adopt compact conformations with a large number of surface reactive groups. The structural formula of HBPE-CA microspheres with $BA_{arm} = 5$ (it meant the five hydroxyl groups of HBPE had undergone carboxylation reaction) was shown in Fig. 1A. The ^1H NMR spectrum of HBPE-CA was shown in Fig. 1B. In the ^1H NMR spectrum of HBPE-CA, new proton signals appeared at 2.51 ppm (protons **d**), which confirmed that butanedioic anhydride was grafted successfully through the formation of ester bondings [28]. The conversion ratio from hydroxyl groups to carboxyl groups could be calculated by comparing the integral of peak d with the integral of peaks a, b and c ($2S_d/3S_{a,b,c}$) is about 41.3%.

The ESI-MS of HBPE and HBPE-CA were shown in Fig. S1. HBPE: 1179 (1202-Na^+). The calculated molecular weight was 1179. The consecutive peaks (273, 389, 505, 621, 737, 853, 969, 1085, 1201) had a distance of 116, which corresponded to the repeat unit $M_{DMPA}–M_{H2O}$, as the red section of illustration of Fig. S1(A).

HBPE-CA microspheres: 1715 (Fig. S1(B)). The calculated molecular weight of HBPE-$(CA)_5$ was 1718. So the real molecular weight was consistent with the calculated molecular weight. It indicated that the conversion ratio from hydroxyl groups to carboxyl groups was 41.7%. The result is in agreement with the datum that was obtained from ^1H NMR spectrum of HBPE-CA microspheres.

TEM was performed to estimate the size and morphology of the HBPE-CA microspheres. Typical TEM photographs of the microspheres showed that HBPE-CA microspheres were well dispersed with an average diameter of 270 nm (Fig. S2).

3.2. Hemocompatibility of the HBPE-CA microspheres

The in vitro blood compatibility was evaluated by coagulation tests and platelet activation. The experimental procedure to evaluate the hemocompatibility of microspheres was described in our previous report [31–33].

Blood clotting is the result of a complex process initiated by the intrinsic system or the extrinsic system and/or a common pathway. As the various coagulation assays indicated the interactions at different stages of the coagulation, they provided basic information about the mode of action of anticoagulants. The antithrombogenicity of the samples was evaluated by in vitro coagulative time tests, activated partial thromboplastin time (APTT), prothrombin time (PT) and thrombin time (TT) tests. Blood was drawn from healthy rabbits containing sodium citrate. The platelet-poor plasma (PPP) was obtained by centrifuging blood at 3000 rpm for 20 min. The final concentration of the test samples mixed with PPP was 1 mg·mL^{-1}. PBS was used as a control. The APTT, PT and TT of control sample for healthy plasma are 16.9 ± 0.1,

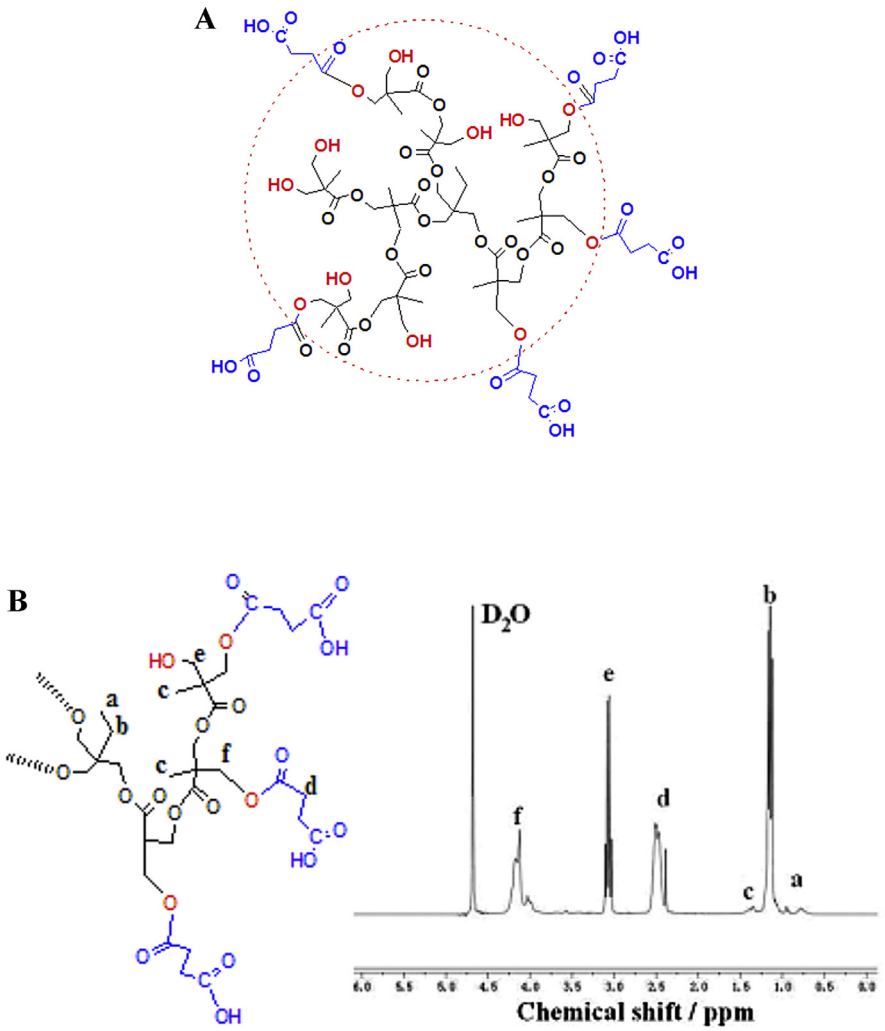

Fig. 1. (A) The chemical structure of HBPE-CA microspheres. (B) ^{1}H NMR spectrum of HBPE-CA microspheres.

8.1 ± 0.1, and 15.9 ± 0.4 s, respectively. As shown in Fig. 2A, the APTT/PT/TT data of HBPE were slightly lower than the data of control, indicating that the HBPE itself had coagulative properties to a certain extent. However, the APTT/PT/TT values of the HBPE-CA microspheres were all higher than that of control. Thus, the HBPE-CA microspheres did not cause the extrinsic pathway of coagulation, meanwhile, the microspheres inhibited both the intrinsic and/or common pathways of coagulation and thrombin activity or conversion of fibrinogen to fibrin. The results demonstrated that the good antithrombogenicity of the HBPE-CA microspheres can be attributed to the pendant functional carboxylic acid groups with negative charge [34,35].

Platelet activation (platelet release, pyridoxamine phosphate formation, P-selectin expression, aggregation) and adhesion are known to occur during cardiopulmonary bypass, hemodialysis, as well as with vascular grafts and catheters [36]. Platelet activation upon interaction with samples is another indication of blood incompatibility as it could lead to thrombotic complications under in vivo conditions. To measure the platelet activation, the platelet rich plasma (PRP) was incubated at 37 °C with an equal volume of the HBPE-CA microspheres suspension where the final samples concentration was 1 mg·mL^{-1}. The incubation mixture was removed at 30 min to assess the activation state of the platelets using fluorescence flow cytometry. Expression of the fluorescently labeled platelet activation marker anti-CD62P and the platelet pan-marker anti-CD42a was detected using flow cytometry. Platelet activation was expressed as the percentage of platelets positive for both of the bound antibodies, anti-CD62P and anti-CD42a. As shown in Fig. 2B, the pristine HBPE sample caused platelet activation in some degree. After modification, the sample exhibited similar activation behavior to that of the control sample, indicating that the HBPE-CA microspheres did not activate platelets.

3.3. Characterization of TBA/(HBPE-CA) hybrids

UV–vis spectroscopy was used to confirm the binding function between TBA and HBPE-CA microspheres. In Fig. 3A, HBPE-CA microspheres showed no absorption peak from 200 to 700 nm. After TBA was attached to the HBPE-CA microspheres, an obvious absorption peak appeared at 260 nm as shown in Fig. 3A, which is a characteristic of the DNA strand, indicating the successful binding between TBA and HBPE-CA microspheres [37].

SEM was used to characterize the stepwise fabrication process of the aptamer biosensor. As shown in Fig. S3(A), the HBPE-CA microspheres displayed a well-dispersed structure in the form of spherical. The diameters of the HBPE-CA microspheres were about 260 nm. The result correlated well with TEM result in Fig. S2. Compared with the image of the HBPE-CA microspheres, the more dense and homogeneous structure could be observed for the TBA/(HBPE-CA)/GCE film (Fig. S3(B-C)), indicating the successful binding between TBA and HBPE-CA microspheres. This uniform

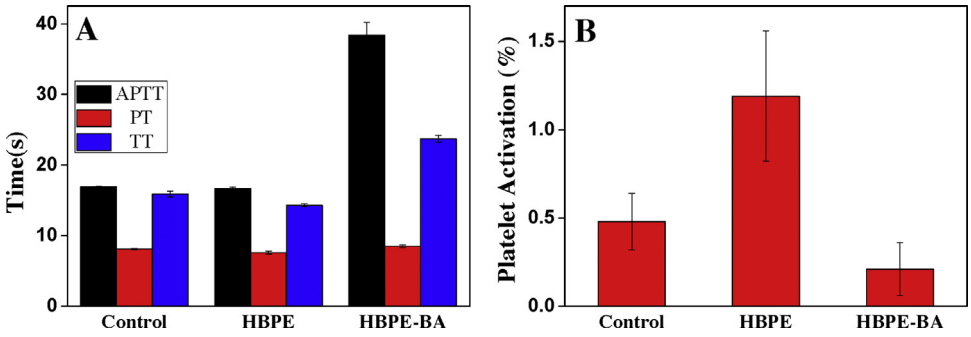

Fig. 2. Hemocompatibility of HBPE-CA microspheres. (A) APTT/PT/TT of 1 mg·mL^{-1} HBPE and HBPE-CA microspheres. PBS was used as a control. (B) Platelet activation upon interaction of 1 mg·mL^{-1} HBPE and HBPE-CA microspheres with PRP for 30 min at 37 °C. Plasma incubated with saline as a negative control. Data are presented as means ± standard deviation (n = 3).

nanostructure provided a significant increase of the effective electrode surface for loading of biomolecules and accelerating electron transfer.

To validate the conformational change of binding interaction, we measure the CD spectra of TBA under different conditions. It is reported that CD can measure the structures and ligand binding of quadruplex DNAs [11,38]. Therefore we investigated the conformation change of TBA before and after the addition of thrombin. It can be seen from curve a in the Fig. 3B that the CD spectra of TBA at room temperature exhibited a negative band centered around 232 nm, and positive band around 249 nm and 294 nm in the absence of the HBPE-CA microspheres [39]. Upon the addition of 1 mg·mL^{-1} HBPE-CA microspheres, three peaks were similar to the pure aptamer in both peak intensity and peak position (curve b). In the presence of 0.1 μM thrombin, the negative peak decreased and shifted to about 224 nm (curve c). With the increasing of thrombin concentrations to 0.2 μM, the negative peak decreased tremendously in CD spectra (curve d), indicating formation of the TBA quadruplex. This is in accordance with the previous report [40]. The results suggested that the G-quadruplex structure of TBA is induced by specific interaction between TBA and thrombin [41]. Thus, HBPE-CA microspheres were crucial for the conformation conversion of aptamer (i.e., change of a single strand in helix conformation to the G-quadruplex form), which attributed to the good biocompatibility of microspheres.

Polyacryl amide gel electroph oresis (PAGE) can be used for the separation and purification of biological macromolecules [42,43]. Especially, high concentration PAGE has a higher resolution in the separation of short DNA fragments. Different molecular mass or different conformation of DNA will appear as different stripes. The PAGE images demonstrating the impact of the binding of HBPE-CA microspheres on the structure of TBA sequence were shown in Fig. S4. It was observed that in the absence of HBPE-CA, one component of TBA were present as shown in Fig. S4. And then, the addition of HBPE-CA microspheres resulted in the fading of single-strand strip of TBA, indicating that HBPE-CA might affect the stabilization of TBA via intercalating into base pairs. Besides, two components were present in Fig. S4. This suggested that due to the interaction, the single-strand TBA would get greater resistance in the electrophoresis assay. Consequently, the mobility of TBA was decreased. The increase of the G-quadruplex (referred as G) mobility in the gel was supposed to be caused by its larger charge and more compact structure than that of single-strand TBA. These observations correlate well with CD results which showed that the binding of HBPE-CA could induce the conversion of DNA structures to the G-quadruplex form, thereby resulting in the formation of complex with decreased mobility.

3.4. Characterization of thrombin/TBA/(HBPE-CA) aptamer biosensor

Since the interaction of thrombin and TBA takes time, the effect of incubation time on sensor response was studied. Fig. S5 showed the dependence of current on incubation time. The plot in Fig. S5 suggested that the current response decreased with the incubation time from 0 to 100 min and reached a plateau after 80 min, suggesting that the association reaction between TBA and thrombin almost reached saturation at 80 min. Nevertheless, considering the urgent time in clinical practice, 20 min is good enough. Thus, 20 min was chosen as the incubation time for following experiments.

In order to evaluate the changes of electrode behavior after each assembly step [44–46], we studied the CV of HBPE-CA microspheres modified ITO (curve a), after immobilization of TBA for 24 h (curve b), and after incubation of the later in thrombin solution for 20 min (curve c). As shown in Fig. 4A, the self-assembly

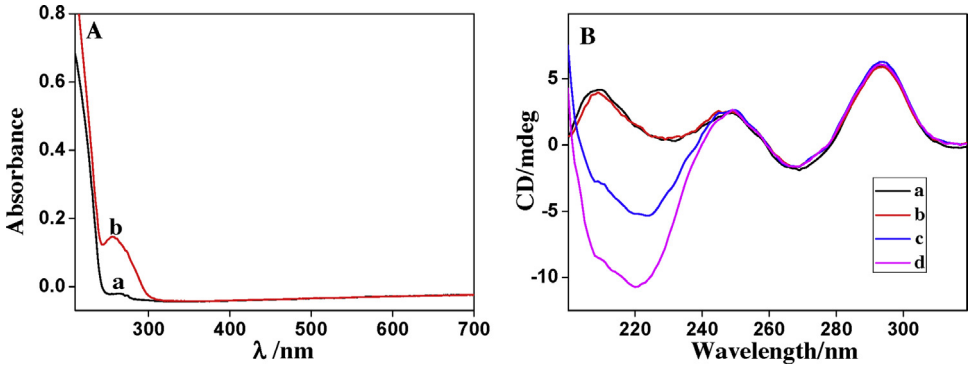

Fig. 3. (A) UV–vis absorption spectra of (a) HBPE-CA microspheres and (b) TBA/(HBPE-CA). (B) CD spectra of (a) TBA, (b) TBA/(HBPE-CA), (c) TBA/(HBPE-CA) with 0.1 μM thrombin and (d) TBA/(HBPE-CA) with 0.2 μM thrombin. Scan speed: 50 nm·min^{-1}, scan range: 200–320 nm.

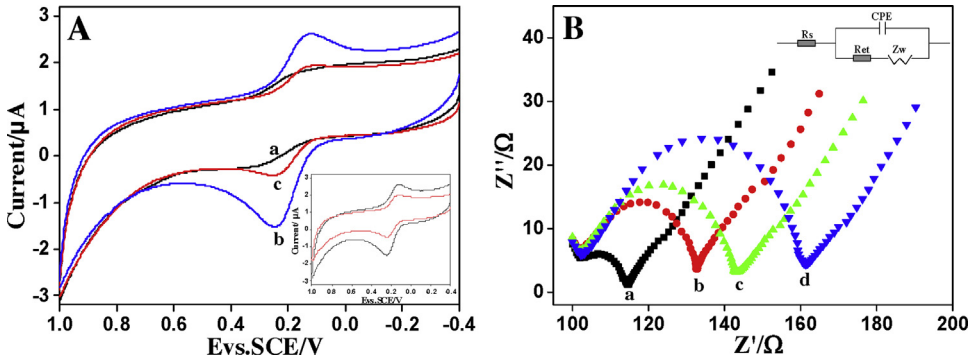

Fig. 4. (A) CVs of (a) HBPE-CA microspheres modified ITO, (b) TBA/(HBPE-CA) modified ITO and (c) thrombin/TBA/(HBPE-CA) modified ITO in 0.10 M PBS (pH 7.4) containing 10 mM $K_3Fe(CN)_6/K_4Fe(CN)_6$ and 0.1 M KCl. The insert was the CVs of TBA/(HBPE-CA) modified ITO (black line), and TBA modified ITO (red line). Scan rate 100 mV s^{-1}. (B) Nyquist plot of Faradic impedance obtained in 0.10 M PBS (pH 7.4) containing 10 mM $K_3Fe(CN)_6/K_4Fe(CN)_6$ and 0.1 M KCl for (a) bare ITO, (b) HBPE-CA microspheres modified ITO, (c) TBA/(HBPE-CA) modified ITO and (d) thrombin/TBA/(HBPE-CA) modified ITO. Inset is a schematic of the equivalent circuit. (For interpretation of the references to color in this figure legend, the reader is referred to the web version of this article.)

of HBPE-CA microspheres onto the ITO electrode resulted in a CV in the shape of a straight line, due to the strong inhibition of the electron migration process caused by the high membrane resistance of HBPE-CA microspheres (curve a). When TBA was grafted onto the (HBPE-CA)/ITO, the modified electrode exhibited a pair of stable and well-defined redox peaks at 0.248 and 0.122 V in 0.10 M PBS (pH 7.4) containing 10 mM $K_3Fe(CN)_6/K_4Fe(CN)_6$ and 0.1 M KCl (curve b), which corresponded to the formation of an organic layer of TBA [11]. Upon incubation with thrombin solution, the peak current decreased greatly (curve c), suggesting an obvious steric hindrance process for the binding of thrombin to the surface of the modified ITO. Comparing TBA/(HBPE-CA) modified ITO (insert of Fig. 4A, black line) with TBA modified ITO (insert of Fig. 4A, red line), we found that the structure of HBPE-CA microspheres can provide high surface to volume ratios and high surface activity, thus possess advantages in terms of TBA immobilization.

As a powerful tool for probing the interface features of surface-modified electrodes, EIS was further used to study the stepwise assembly of the aptamer biosensor. The impedance spectra include a semicircle portion and a linear portion. The semicircle portion at higher frequencies corresponds to the electron-transfer limited process, and the linear portion at lower frequencies represents the diffusion-limited process. The semicircle diameter equals to the electron-transfer resistance (R_{et}). Fig. 4B illustrated the Nyquist plots of EIS for the different modified electrodes in presence of redox probe, $[Fe(CN)_6]^{3-/4-}$. At a bare ITO, the redox process of the probe showed an electron-transfer resistance of about 12.6 Ω (curve a), while the HBPE-CA microspheres modified ITO electrode showed a higher resistance for the redox probe (curve b), implying that the access of the redox probes to the electrode surface would be hindered. In the case of TBA/(HBPE-CA)/ITO (curves c), the resistance further increased because of the contribution of assembled TBA. When thrombin was assembled on the TBA/(HBPE-CA)/ITO, the resistance increased greatly (curve d), owing to the dielectric behavior of thrombin for interfacial electron transfer processes and blocked the electron exchange between the redox probe and the electrode. The results were consistent with the observation from SEM images as shown in Fig. S3. Thus, we might conclude that the HBPE-CA film not only offered a biocompatible surface for protein loading and protein capture but also provided a sensitive electric interface for further sensing.

DPV technique has a potential advantage to increase the sensitivity and selectivity in the process of detection [47]. Fig. 5A showed DPV curves recorded on the TBA/(HBPE-CA)/ITO in the presence of various thrombin concentrations in whole blood. Blood samples were supplied by volunteers. Fig. 5B showed the calibration curve obtained by measuring the DPV peak current intensity vs. logarithmic value of thrombin concentration. The measurements were repeated 3 times to obtain the standard deviation. A linear relationship between the current intensity and logarithmic value of thrombin concentration could be found in the range of 10 fM–100 nM in whole blood. The linear regression equation was I (μA) = −0.26 log$c$ −1.58 with a correlation coefficient of 0.9961 (n = 10). The apparent surface of the electrode is estimated to be about 0.033 cm^2, and the sensitivity was calculated to be 0.78 μA M^{-1} cm^{-2}. The detection limit for thrombin concentration was estimated to be 0.90 fM (S/N = 3),

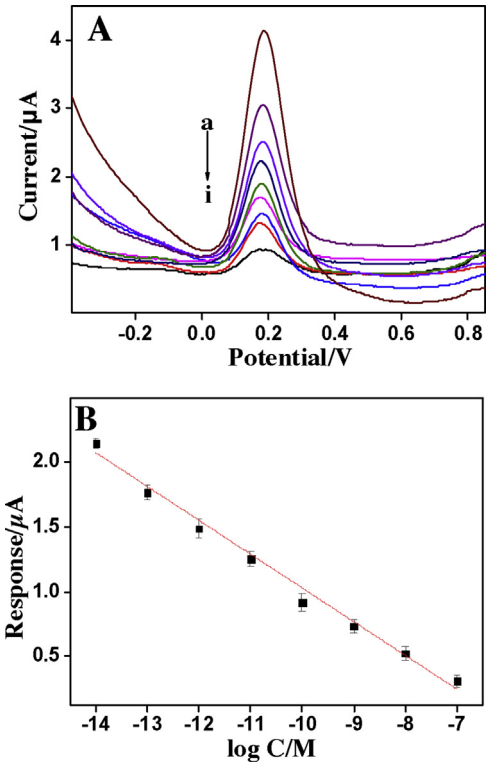

Fig. 5. The relationship between the current response and α-thrombin concentration in whole blood. (A) The concentration of thrombin was (a) 0, (b) 10 fM, (c) 100 fM, (d) 1 pM, (e) 10 pM, (f) 100 pM, (g) 1 nM, (h) 10 nM and (i) 100 nM in 0.10 M PBS (pH 7.4) containing 10 mM $K_3Fe(CN)_6/K_4Fe(CN)_6$ and 0.1 M KCl. (B) The calibration curve between the current response and thrombin concentration (logarithm).

which was much lower than the detection limit recently reported using GR fluorescence aptasensor [48] and electrochemical thrombin sensors [49].

The reproducibility of the aptamer biosensor was evaluated from the DPV response of the thrombin/TBA/(HBPE-CA) modified ITO electrode. A series of six measurements from the batch resulted in a relative standard deviation (RSD) of 5.4%, indicating good electrode-to-electrode reproducibility of the fabrication protocol described above. On the other hand, the intra-assay precision of the aptamer biosensor was estimated by assaying two thrombin concentrations for six replicate measurements. At the thrombin concentrations of 10 pM and 50 pM, the RSDs of intra-assay with this method were 6.5% and 6.8%, showing an acceptable precision. Since stability is a very important characteristic, it was necessary to check it for the developed aptamer biosensor here. When the thrombin/TBA/(HBPE-CA) modified ITO electrode was stored in the refrigerator at 4 °C within a storage period of 20 days, the DPV response retained 92.8% value of the initial response, showing a quite satisfying stability. Good stability can be attributed to the strong interactions between TBA and thrombin. In addition, to examine the repeated use of the aptamer biosensor, the aptamer electrode was rinsed with 7 M urea solution, and annealed at 90 °C for 1 min. After the treatment, the aptamer was incubated with thrombin solution again and subsequently washed, and the signal change was observed before and after target binding. We repeated the same experiment four times. Then, till the third time, 90% of its original activity was recovered, and clear signal changes could be observed, indicating that the aptamer biosensor can be simply and functionally reactivated.

3.5. Interference

For testing the specific recognition to thrombin of the aptamer biosensor designed, bull serum albumin (BSA) and lysozyme which are usually used in control experiments, were adopted [50]. The modified ITO electrode was immersed in the solution of 1 μM BSA and 1 μM lysozyme for 30 min without the presence of thrombin, respectively. Relative response in Fig. 6 was obtained by signals of the proteins dividing the signal of the thrombin then multiplying 100%. It was found that BSA and lysozyme had almost no interference with the determination of thrombin, indicating that these species coexisting in the sample matrix did not affect the determination of thrombin and the aptamer biosensor had a good specificity.

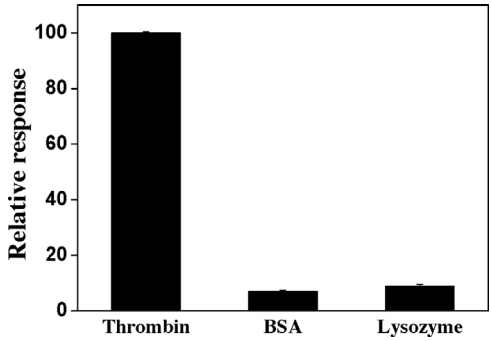

Fig. 6. Detecting specificity in a solution containing 1 μM BSA, 1 μM lysozyme and 0.01 μM of thrombin. It is an average value of the response of three measurements for each sample.

Table 1
Determination of thrombin concentrations in whole blood samples using the thrombin/TBA/(HBPE-CA) aptamer biosensor.

No.	Determined by the aptamer biosensor		Measured by fluorescence	
	Concentrations (nM)	RSD (%)	Concentrations (nM)	RSD (%)
1	9.58	4.36	10.14	3.72
2	36.16	5.53	36.98	4.81
3	49.04	4.32	49.86	4.65
4	53.15	5.89	53.97	3.58
5	63.83	4.51	65.48	5.20

The data were average values of five measurements for each sample.

3.6. Real sample analysis

To evaluate its applicability, the aptamer biosensor was used for determination of the concentration of thrombin in whole blood. Five blood samples obtained from hospital were analyzed by using five independently prepared biosensors. The obtained results were compared with those measured in serum samples with fluorescence method (Table 1) [30]. It showed that the values measured in whole blood by the developed aptamer biosensor were in good agreement with the data measured in serum samples which are isolated from whole blood. Furthermore, in consideration of centrifugation process and serum determination, we have reason to believe that the results measured in whole blood by the developed aptamer biosensor are closer to the actuals. Thus, the aptamer biosensor can be used for the thrombin detection in whole blood sample and further investigation will be done by our research group in near future.

4. Conclusions

Analysts are always enthusiastic about finding new materials with good biocompatibility to improve the behavior of biosensors. In this case, the water-soluble HBPE-CA microspheres were synthesized successfully, and then a label-free and sensitive thrombin aptamer biosensor based on the HBPE-CA microspheres was prepared and applied in whole blood directly. To the best of our knowledge, this is the first time that the hyperbranched polymer microspheres functionalized by carboxylic acid groups have been utilized to prepare a novel aptamer biosensor which is suitable for thrombin detection in whole blood directly. The integration of the technologies, which includes anticoagulant, sensor and nanoscience, will bring significant input to high-performance biosensors relevant to diagnostics and therapy of interest for human health.

Acknowledgments

The work is supported by Major Program for the Natural Science Fundamental Research of the Higher Education Institutions of Jiangsu Province (12KJA150006), the Priority Academic Program Development of Jiangsu Higher Education Institutions, and Base of production, education and research of prospective joint research project of Jiangsu Province (BY2011109).

Appendix A. Supplementary data

Supplementary data associated with this article can be found, in the online version, at http://dx.doi.org/10.1016/j.aca.2014.08.010.

References

[1] S. Centi, S. Tombelli, M. Minunni, M. Mascini, Anal. Chem. 79 (2007) 1473.
[2] M.A. Shuman, P.W. Majerus, J. Clin. Invest. 58 (1976) 1258.
[3] M. Oroval, E. Climent, C. Coll, R. Eritja, A. Aviñó, M.D. Marcos, F. Sancenón, R. Martínez-Máñez, P. Amorós, Chem. Commun. 49 (2013) 5482.
[4] A. Erdem, H. Karadeniz, G. Mayer, M. Famulok, A. Caliskan, Electroanalysis 21 (2009) 1284.
[5] S. Centi, G. Messina, S. Tombelli, I. Palchetti, M. Mascini, Biosens. Bioelectron. 23 (2008) 1609.
[6] J. Hu, P.C. Zheng, J.H. Jiang, G.L. Shen, R.Q. Yu, G.K. Liu, Anal. Chem. 81 (2009) 93.
[7] Y. Wang, H. Wei, B. Li, W. Ren, S. Guo, S. Dong, E. Wang, Chem. Commun. 28 (2007) 5222.
[8] T. Hermann, D.J. Patel, Science 287 (2000) 825.
[9] M. Luzi, S. Minunni, Trends Anal. Chem. 22 (2003) 818.
[10] A. Bourdoncle, C. Estevez-Torres, L. Gosse, P. Lacroix, T. Vekhoff, L. LeSaux, J.L. Mergny, J. Am. Chem. Soc. 128 (2006) 11105.
[11] G.S. Bang, S. Cho, B.G. Kim, Biosens. Bioelectron. 21 (2005) 870.
[12] S.H. Choum, K.H. Chin, A.H. Wang, Trends Biochem. Sci. 30 (2005) 234.
[13] F. Le Floch, H.A. Ho, M. Leclerc, Anal. Chem. 78 (2006) 4731.
[14] M. Zayats, Y. Huang, R. Gill, C.A. Ma, I. Willner, J. Am. Chem. Soc. 128 (2006) 13667.
[15] J.J. Li, Y. Chu, B.Y. Lee, X.S. Xie, Nucleic Acids Res. 36 (2008) e36.
[16] E.S.Q. Tan, R. Wivanius, C.S. Toh, Electroanalysis 21 (2009) 754.
[17] H. Cai, T.M.H. Lee, I.M. Hsing, Sens. Actuators B 114 (2006) 437.
[18] H. Yang, J. Ji, Y. Liu, J. Kong, B. Liu, Electrochem. Commun. 11 (2009) 40.
[19] Y. Wang, Y. Xiao, X. Ma, N. Li, X. Yang, Chem. Commun. 48 (2012) 740.
[20] Y.B. Kim, H.K. Kim, H. Nishida, T. Endo, Macromol. Mater. Eng. 289 (2004) 926.
[21] M. Ahmed, R. Narain, Biomaterials 33 (2012) 4001.
[22] Y.L. Xiao, H. Hong, A. Javadi, J.W. Engle, W.J. Xu, Y.A. Yang, Y. Zhang, T.E. Barnhart, W.B. Cai, S.Q. Gong, Biomaterials 33 (2012) 3082.
[23] D. Foix, A. Serra, L. Amparore, M. Sangermano, Polymer 53 (2012) 3088.
[24] X.Y. Zhu, L. Chen, D.Y. Yan, Q. Chen, Y.F. Yao, Y. Xiao, J. Hou, J.Y. Li, Langmuir 20 (2004) 490.
[25] D.L. Wang, H.Y. Chen, Y. Su, F. Qiu, L.J. Zhu, X.Y. Huan, B.S. Zhu, D.Y. Yan, F.L. Guo, X.Y. Zhu, Polym. Chem. 4 (2013) 94.
[26] X.H. He, X.M. Wu, X. Cai, S.L. Lin, M.R. Xie, X.Y. Zhu, D.Y. Yan, Langmuir 28 (2012) 11938.
[27] J.Y. Liu, Y. Pang, J. Chen, P. Huang, W. Huang, X.Y. Zhu, D.Y. Yan, Biomaterials 33 (2012) 7774.
[28] N.E. Ikladious, J.N. Asaad, N.N. Rozik, Des. Monomers Polym. 12 (2009) 481.
[29] S. Sam, L. Touahir, J. Salvador Andresa, P. Allongue, J.N. Chazalviel, A.C. Gouget-Laemmel, C. Henry de Villeneuve, A. Moraillon, F. Ozanam, N. Gabouze, S. Djebbar, Langmuir 26 (2010) 814.
[30] Y. Jin, J. Bai, H. Li, Analyst 135 (2010) 1735.
[31] C. Sun, L. Chen, F. Xu, P. Zhu, J. Luan, C. Mao, J. Shen, J. Mater. Chem. B 1 (2013) 809.
[32] H. Hu, X.B. Wang, S.L. Xu, W.T. Yang, F.J. Xu, J. Shen, C. Mao, J. Mater. Chem. 22 (2012) 15369.
[33] C. Mao, L.C. Jiang, W.P. Luo, H.K. Liu, J.C. Bao, X.H. Huang, J. Shen, Macromolecules 42 (2009) 9368.
[34] Z.Q. Zhang, S.A. McCallum, J. Xie, L. Nieto, F. Corzana, J. Jimenez-Barbero, M. Chen, J. Liu, R.J. Linhardtt, J. Am. Chem. Soc. 130 (2008) 13007.
[35] B.C. Dash, G. Réthoré, M. Monaghan, K. Fitzgerald, W. Gallagher, A. Pandit, Biomaterials 31 (2010) 8197.
[36] V.M. Walley, W.A. Stinson, C. Upton, J.P. Santerre, T. Mussivand, R.G. Masters, F. N. Ghadially, Cardiovasc. Pathol. 2 (1993) 185.
[37] H. Liu, S. Xu, Z. He, A. Deng, J.J. Zhu, Anal. Chem. 85 (2013) 3392.
[38] B.I. Kankia, L.A. Marky, J. Am. Chem. Soc. 123 (2001) 10804.
[39] H. Ito, S. Tanaka, M. Miyasaka, Biopolymers 65 (2002) 80.
[40] S. Nagatoishi, Y. Tanaka, K. Tsumoto, Biochem. Biophys. Res. Commun. 352 (2007) 817.
[41] Y. Jin, H. Li, J. Bai, Anal. Chem. 81 (2009) 5715.
[42] E.A. Lewis, M. Munde, S. Wang, M. Rettig, V. Le, V. Machha, W.D. Wilson, Nucleic Acids Res. 22 (2011) 9658.
[43] T. Kaneta, T. Ogura, S. Yamato, T. Imasaka, J. Sep. Sci. 35 (2012) 435.
[44] S. Bharathi, M. Nogami, S. Ikeda, Langmuir 17 (2001) 4.
[45] J. Jia, B. Wang, A. Wu, G. Cheng, Z. Li, S. Dong, Anal. Chem. 74 (2002) 2223.
[46] R. Liang, J. Qiu, P. Cai, Anal. Chim. Acta 534 (2005) 229.
[47] W.C. Liao, J. Ho, Anal. Chem. 81 (2009) 2476.
[48] H. Chang, L. Tang, Y. Wang, J. Jiang, J. Li, Anal. Chem. 82 (2010) 2346.
[49] T. Sun, L. Wang, N. Li, X. Gan, Bioproc. Biosyst. Eng. 34 (2011) 1085.
[50] Y. Li, L. Liu, X. Fang, J. Bao, M. Han, Z. Dai, Electrochim. Acta 65 (2012) 6.